JOURNAL OF APPLIED ELECTROCHEMISTRY 27 (1997) 19–24

Preparation and characterization of matrices for phosphoric acid fuel cells

M. I. CAIRES, M. L. BUZZO, E. A. TICIANELLI, E. R. GONZALEZ

Instituto de Química de São Carlos/USP, CP 780, 13560-970 São Carlos, SP, Brazil

Received 2 January 1996; revised 4 April 1996

In this work results on the preparation, characterization and single cell testing of matrices for phosphoric acid fuel cells are reported. The matrices were produced using mixtures of powders of silicon carbide with zirconium silicate or niobium carbide, by deposition of an aqueous emulsion of the powders on top of the catalyst layer of the gas diffusion electrodes, or by making a self-supported film of the materials. The physical characterization of the powders and of the matrices included the distribution of particle size and shape of the powders and the thickness, electrical resistance, and pore size distribution in the matrices. The matrices were evaluated under operation, using standard supported platinum on carbon gas diffusion electrodes in a H_2/O_2 single fuel cell setup operating with phosphoric acid at 180°C. The results of the cell potential–current density characteristics were analysed to separate the contribution of the structural properties of the matrices on the total polarization losses of the single cells. It was found that a single cell operating with a self-supported matrix composed of 50 wt % NbC + SiC has a much better performance than that observed with SiC alone.

1. Introduction

The most advanced fuel cell technology is that based on a phosphoric acid electrolyte (PAFC) operating at around 200°C with hydrophobic electrodes prepared with platinum on carbon catalysts. In such a system the liquid electrolyte is placed between the electrodes embedded on a supporting porous matrix fabricated with highly chemically inert and electronic insulating materials. In the fuel cell the electrolyte/matrix composite is used to provide the ionic conductivity, to avoid short-circuiting of the electrodes and to minimize crossover of the reactant gases. Also, the physicochemical properties of the composite matrix should be adequate in order to guarantee that the bulk liquid electrolyte is permanently immobilized inside the cell providing the optimized amount required for the cell reactions in the triple phase reaction zone. At the same time the matrix must not permit flooding, in one extreme, or the interruption of current conduction by drying, in the other, under operational conditions.

Silicon carbide (SiC) mixed with a small amount (around 2 wt %) of polytetrafluoroethylene (PTFE) is the most commonly reported material used for the preparation of the matrix for phosphoric acid [1, 2]. To form the matrix, a layer of about 100 μm thickness of the material is applied on the catalyst layer of the cathode by a screen-printing method. The matrix layer is subsequently filled with the electrolyte.

More recently, other than the conventional materials and matrix preparation procedures have been employed [3, 4] for the retention of the electrolyte in PAFC, using mixtures of SiC with several metal carbides [3] or metal silicides [4], a plasticizer and PTFE to prepare a thin layer of a self-supported matrix. To assemble the cell the resulting foil is flooded with the electrolyte and sandwiched between a pair of electrodes. However, to date there are no reports on the performance of such materials.

In this work results on the preparation, characterization and single cell testing of composite phosphoric acid fuel cell matrices are reported. The matrices were prepared using mixtures of powders of silicon carbide (SiC) with zirconium silicate ($ZrSiO_4$) or niobium carbide (NbC), by two different methods: (i) deposition of an aqueous emulsion of the powders on the catalyst layer of the gas diffusion electrodes by a screen-printing procedure and (ii) fabrication of a self-supported film of the materials by a hot rolling technique.

2. Experimental details

Polarographic analyses of the solution resulting from acid treatment of the NbC (CBMM, Brazil) and $ZrSiO_4$ (Nuclemon, Brazil) raw powders indicated as contaminants C, Cu, Pb, Cd, Ni, Co, and Fe below 1 ppm while for SiC (Carborundum, Brazil) the levels were of the order of 5–8 ppm. These materials were purified by treatment at high temperature (1000°C, 1 h) in air and boiling in aqua regia for about 48 h followed by extensive water rinsing. The physical characterization of the powders included the determination of the distribution of particle size and shape for the SiC, NbC and $ZrSiO_4$ using scanning electron microscopy (SEM: Cambridge Stereoscan, model S4-10) and photon correlation spectroscopy (PCS: Brookhaven Instruments Co., model 2030).

0021-891X

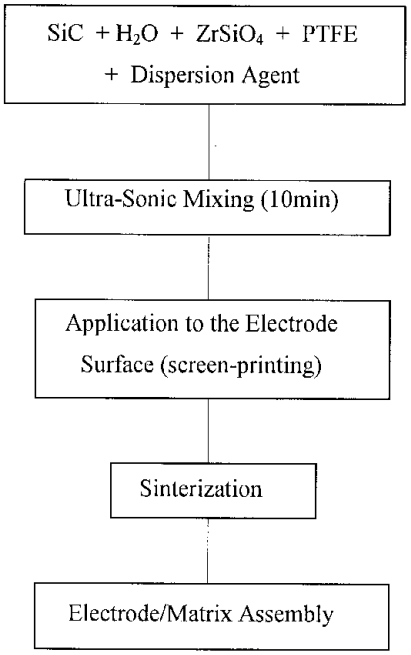

Fig. 1. Block diagram for matrix preparation using the screen-printing method.

The fuel cell matrices were prepared by screen-printing and rolling techniques according to the procedures described schematically in Figs 1 and 2. With pure SiC and SiC/$ZrSiO_4$ mixtures, satisfactory matrices could only be obtained using the screen-printing method. Attempts to prepare self-supported films of these materials were not successful due to lack of mechanical integrity. On the other hand, with SiC/NbC mixtures of the powders, in the composition range of 20–50 wt % SiC, it was possible to build mechanically stable films.

The finished matrices (screen-printing SiC, SiC/NbC and SiC/$ZrSiO_4$, and self-supported SiC/NbC) were characterized by the following properties:

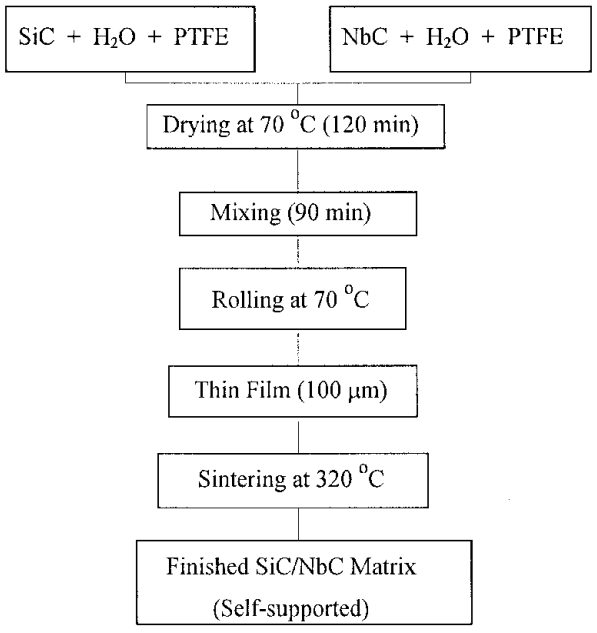

Fig. 2. Block diagram for self-supported matrix preparation using the rolling process.

(i) thickness, which was measured using a thickness gauge (Elcameter),
(ii) electrical resistivity, measured by placing the two faces of the substrate in contact with mercury and using the two probe ohmic effect technique,
(iii) pore size distribution, measured using a Micromeritics pore sizer (model 9310),
(iv) rate of electrolyte penetration, determined by measuring the propagation of the wet boundary along the surface of the matrix, after placing one of the edges in contact with 85% H_3PO_4 at room temperature.

Testing of the performance of the matrices in phosphoric acid single cells was carried out using standard supported platinum on carbon gas diffusion electrodes with a catalyst loading of 0.4 mg Pt cm^{-2}. The electrodes, with a geometric active area of 4.0 cm^2, were prepared as described elsewhere [5] using a hydrophobic carbon paper substrate. The single cell was operated with H_2/O_2 at 1 atm, in 98% (w/w) phosphoric acid and in a temperature of 180°C.

3. Results and discussion

Figure 3 shows examples of the SEM micrographs while Table 1 summarizes the results obtained for the distribution of particle size and shape of the SiC, NbC and $ZrSiO_4$ powders. Tables 2 and 3 summarize the physical characteristics of the different matrices, presenting the values of the pore size distribution, rate of electrolyte penetration, thickness and electrical resistivity. The data presented for the composite matrices are those obtained for the compositions and configurations which showed the best performance for fuel cell operation.

The results in Table 2 show that the average pore size of the matrices prepared with mixtures of powders are about one order of magnitude smaller than for matrices prepared with pure SiC. These results can be explained in terms of the shapes and the average

Table 1. Distribution of particle size and shape of the SiC, NbC and $ZrSiO_4$ powders

Powder	*Average particle size* /μm	*Shape*
SiC	5.5	sharp needles
NbC	2.2	spherical particles
$ZrSiO_4$	2.0	spherical particles

Table 2. Pore size distribution and electrolyte penetration in the matrices

Matrix	*Average pore size* /μm	*Rate of electrolyte penetration* /cm min^{-1}
SiC + $ZrSiO_4$ (60 wt % SiC) (screen-printing)	0.46	0.08
SiC + NbC (50 wt % SiC) (self-supported)	0.35	0.15
SiC (screen-printing)	2.6	0.10

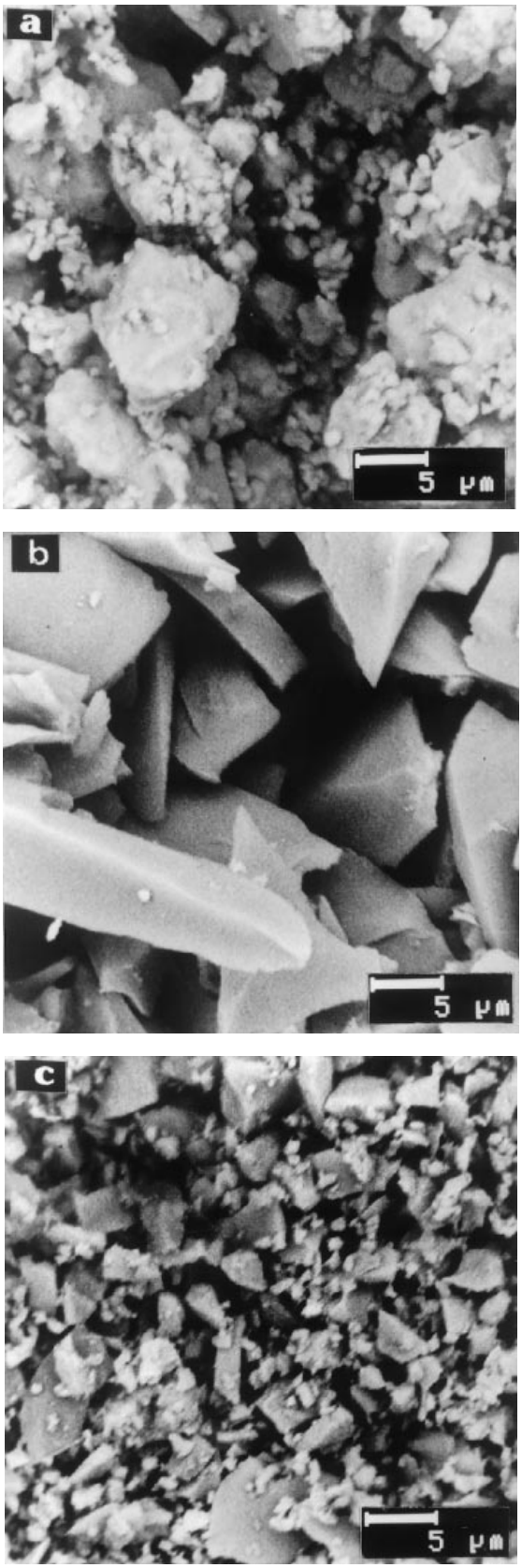

Fig. 3. Scanning electron microscopy of the (a) NbC, (b) SiC and (c) $ZrSiO_4$ powders. Materials were metallized with gold.

particle diameters of the powders employed in the matrix fabrication. In Fig. 3 it is seen that in SiC powder the particles appear as sharp crystals, while in NbC and $ZrSiO_4$ they are rounded as indicated in Table 1. It was also found that the average particle size is close to 5 μm for SiC and only half this value for NbC and $ZrSiO_4$. From these observations it is concluded that in the pure SiC matrix, the particles are arranged in a less compact network, which is compatible with the structure of the material. In the composite matrices the void spaces between the SiC particles are filled with the smaller spherical particles of the other component, resulting in a pronounced decrease of the average pore size. This explanation is also consistent with the observation that a much smaller pore size is formed in the composite material when the particles of the second component are smaller, in particular when NbC is considered.

Table 3. Thickness and electrical resistivity of the matrices

Matrix	*Thickness* /μm	*Range of dry resistivity* /$10^8\ \Omega$ cm
SiC + $ZrSiO_4$ (60 wt % SiC) (screen-printing)	100	6–7
SiC + NbC (50 wt % SiC) (self-supported)	120	1–6
SiC (screen-printing)	100	5–11
SiC + NbC (50 wt % SiC) (screen-printing)	120	2–10

Another important fact observed from the results in Table 2 is that the rate of electrolyte penetration is similar for the pure SiC and SiC/$ZrSiO_4$ matrices, while a higher value is observed for the SiC/NbC composite. This behaviour can be analysed taking into account that the rate of electrolyte penetration is controlled by the hydrostatic pressure drop, which increases with the decrease of pore size and with the increase of hydrophilicity of the materials [6]. If the data in Table 2 are substituted in the hydrostatic pressure drop equation [6] it is concluded that the hydrophilicity changes according to the sequence SiC > SiC/NbC > SiC/$ZrSiO_4$. Thus, the similar rate of electrolyte penetration observed for the SiC and SiC/$ZrSiO_4$ matrices is the result of a compromise with respect to their different characteristics regarding pore size and the hydrophilicity of the materials. For the SiC/NbC matrix the effect of pore size is predominant in determining the rate of electrolyte penetration.

From Table 3 it is observed that the magnitudes of the values of the thickness and of the electronic conductivity of the dry matrices (without impregnation with H_3PO_4) are appropriated for utilization in fuel cells. In principle, the high values of the resistivities will ensure the absence of short circuits, while the thicknesses are low enough to anticipate a small effect of the potential drop due to electrolyte resistance during fuel cell operation with the electrolyte impregnated matrix.

Figure 4 shows the cell potential versus current density characteristics for the H_2/O_2 single cells assembled with the SiC/$ZrSiO_4$ electrolyte matrices prepared using the screen-printing technique. Figure 5 shows the corresponding results obtained for the self-supported SiC/NbC matrices. Figure 6 shows a

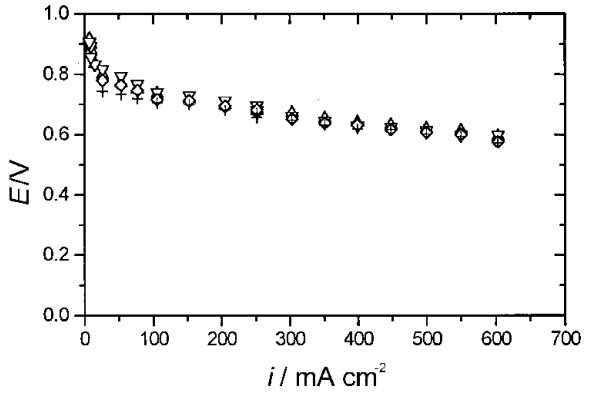

Fig. 4. Cell potential–current density characteristics for H_2/O_2 single cells with different matrices: (+) 70 wt % $ZrSiO_4$; (◇) 60 wt % $ZrSiO_4$; (▽) 40 wt % $ZrSiO_4$ and (△) 30 wt % $ZrSiO_4$ in the screen-printing $SiC/ZrSiO_4$ matrices. PAFC, $T = 180\,°C$.

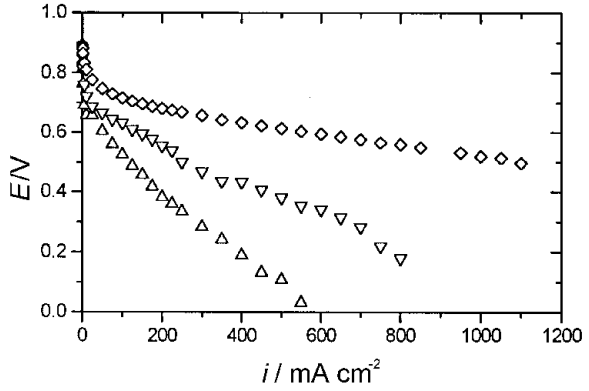

Fig. 5. Cell potential–current density characteristics for H_2/O_2 single cells with different matrices: (△) 80 wt % NbC; (▽) 40 wt % NbC and (◇) 50 wt % NbC in the self-supported SiC/NbC matrices. PAFC, $T = 180\,°C$.

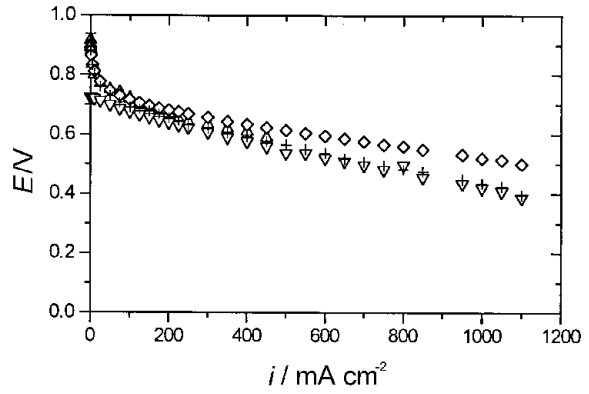

Fig. 6. Cell potential–current density characteristics for H_2/O_2 single cells with different matrices: (▽) screen-printing SiC/NbC (50 wt % SiC); (+) screen-printing SiC (100 wt %); (△) screen-printing $SiC/ZrSiO_4$ (60 wt % SiC); (◇) self-supported SiC/NbC (50 wt % SiC). PAFC, $T = 180\,°C$.

comparison of the cell potential versus current density characteristics for the single cell equipped with the best matrices formed by pure SiC (screen-printing), a mixture of 60 wt % of SiC and $ZrSiO_4$ (screen printing), and 50 wt % SiC and NbC (screen printing and self-supported). Finally, it should be mentioned that the SiC/NbC matrices made by screen-printing gave similar results for all compositions.

The linear region of the polarization diagrams observed at the higher current densities in Fig. 4, shows that the performance of the fuel cell is similar with the different compositions of the screen-printing $SiC/ZrSiO_4$ matrices. On the other hand, the fuel cell behaviour is very different for the different compositions of the self-supported SiC/NbC matrices (Fig. 5). Also, it is seen that for the screen-printing $SiC/ZrSiO_4$ matrices with low contents of SiC, the cell potentials at low current densities are too low. This is also the case for all compositions of the screen-printing SiC/NbC matrix. On the other hand, the self-supported SiC/NbC matrix shows good characteristics near the open circuit cell potential.

The characteristics of the curves presented in Figs 4 to 6 can be interpreted in the following terms:

(i) the small cell potentials observed at low current densities for all the screen-printing SiC/NbC matrices or the $SiC/ZrSiO_4$ containing small amounts of SiC can be explained by the presence of short-circuits in the electrode [7] and/or the presence of gas crossover, probably resulting from the squeeze of the matrix during cell assembly. These problems are not serious, since the effect is restricted to low current densities, and it is associated with a poor mechanical resistance of the composite films or with the presence of pinholes (zones in the matrix not filled with the electrolyte);

(ii) the above effects are not observed for the self-supported SiC/NbC matrices, thus indicating a better uniformity and overall mechanical properties of this material;

(iii) the low, constant values of the slopes of the cell potential–current density characteristics observed at the higher current densities for the $SiC/ZrSiO_4$ matrices show that for this material the ohmic drop is independent of composition. This is probably a consequence of a high capacity of electrolyte retention of the matrices, which is also independent of the composition;

(iv) for the self-supported SiC/NbC matrices at the higher current densities there is a pronounced variation of the slopes of the curves with the composition of the matrix. In this case the behaviour can be explained in terms of wider variation of the capacity for electrolyte retention as a function of the composition, related to the presence of NbC.

In summary, the results of Fig. 6 show that for current densities up to $500\,mA\,cm^{-2}$ the PAFC presents better characteristics when equipped with the composite matrices formed by mixing about 60 wt % of SiC and $ZrSiO_4$ or 50 wt % SiC and NbC. In order to carry out a quantitative comparison of these results, including also those obtained with pure SiC, the experimental single cell polarization data were analysed using the semi-empirical equation proposed by Srinivasan and coworkers [8–10] for the representation of the potential difference of the cell (E) against current density (i) characteristics:

$$E = E^\circ - b \log i - Ri \qquad (1)$$

where

$$E^\circ = E^r + b \log i_\circ \qquad (2)$$

E^r is the reversible potential difference of the cell, b is

Table 4. Kinetic parameters obtained from the fitting of Equation 1 to the experimental polarization results

Matrix	E° *vs RHE* / V	b /mV dec^{-1}	R /Ω cm^2
SiC + $ZrSiO_4$ (60 wt % SiC) (screen-printing)	0.918	86	0.24
SiC + NbC (50 wt % SiC) (self-supported)	0.962	88	0.40
SiC (screen-printing)	0.886	88	0.35

the Tafel slope and $i_\circ$ is the exchange current density of the oxygen reduction reaction (ORR) in the Pt/C catalyst, and R represents mostly the resistance of the matrix/electrolyte in the cell. Small contributions to the values of R are also given by the charge transfer resistance of the hydrogen oxidation reaction (HOR) and the linear diffusion terms due to diffusion problems of the reactant gases in the electrode [10]. Due to the boundary conditions of the present experiments, the two last contributions to R can be considered negligible in the range where Equation 1 is applicable.

Fitting of the above equation to the experimental results was made by a nonlinear least squares method using the experimental data, but it must be stressed that only potentials above 0.7 V were considered. Table 4 shows the values obtained for the kinetic parameters E° and b and R for the three experimental situations under comparison.

The values of E° in Table 4 indicate that the better performance obtained in the low current density region for the 60 wt % SiC/$ZrSiO_4$ and the 50 wt % SiC/NbC matrices can be attributed to a smaller incidence of gas crossover or short circuits in the cell as compared with pure SiC, as already discussed. From the values of E°, it is also observed that these problems, if present, are less important in the case of the self-supported SiC/NbC matrix as compared with SiC/$ZrSiO_4$. On the other hand, the values of R show that the ohmic drop decreases in the sequence SiC/NbC > SiC > SiC/$ZrSiO_4$. Since the thicknesses of the matrices are practically the same (Table 3), this fact could only be related to a higher capacity of electrolyte retention promoted by $ZrSiO_4$, as discussed above. On the other hand, if the whole range of potential covered in Fig. 6 is considered, it is obvious that resistive and/or diffusion effects at high current densities are less important for the SiC/NbC matrix.

The results of Table 4 show that the Tafel slopes of the ORR are very close to 90 mV dec^{-1} for all three cases. These results are a good indication that the mechanism of the ORR is the same in the presence of the different matrices, with the reaction occurring under Temkin adsorption conditions for which the expected Tafel slope of the ORR in the Pt/C catalyst is 2.303 (RT/F) [11–13].

As a final remark, an important practical point can be raised regarding the performance shown in Fig. 6 for the PAFC with the self-supported 50 wt % SiC/NbC matrix. It is observed that current densities above 1000 mA cm^{-2} can be reached at very reasonable cell potentials and with the gases supplied under atmospheric pressure. This performance is very close to that of a polymer electrolyte fuel cell [7]. This is an excellent result because the latter is usually considered to have better power output than the PAFC. However, it must be stressed that, according to Fig. 5, the results are very sensitive to the composition of the matrix.

4. Conclusion

It is observed that in the matrix formed with pure SiC powder, the particles are arranged in a loose structure which is compatible with the size and shape of the particles. In the composite matrices formed with SiC/NbC or SiC/$ZrSiO_4$, the spaces between the SiC particles are filled with the smaller round particles of the other components, resulting in a pronounced decrease of the average pore size. However, it is seen that this property is not the only effect controlling the rate of electrolyte penetration in the matrix, which is also strongly affected by the hydrophobicity of the materials.

The electrochemical results show that the PAFC presents better performance when equipped with the composite matrices formed by mixing about 60 wt % of SiC and $ZrSiO_4$ or 50 wt % SiC and NbC. The trends in the values of E° and R indicate that this behaviour can be attributed to a smaller gas crossover and electrode short-circuiting effects appearing in the SiC/NbC matrix and to a smaller electrolyte resistance introduced by the screen-printing SiC/$ZrSiO_4$ matrix. There is also a good indication that the mechanism of the ORR is the same in all three situations, with the reaction occurring under Temkin adsorption conditions at low current densities. The performance of the PAFC with the self-supported 50 wt % SiC/NbC matrix is very close to that of a polymer electrolyte fuel cell [7] which is an interesting aspect to consider in the comparison of the two technologies.

Acknowledgement

The authors with to thank the Fundação de Amparo a Pesquisa do Estado de São Paulo (FAPESP), Conselho Nacional de Desenvolvimento Científico e Tecnológico (CNPq) and Financiadora de Estudos e Projetos (FINEP) for financial assistance.

References

[1] S. Srinivasan, *J. Electrochem. Soc.* **136** (1989) 41C–48C.
[2] R. D. Breanet, *US Patent 4 017 664* (1977).
[3] K. Takahashi, *Jpn. Pat. Appl. 1-89153 (A)* (1987).
[4] *Idem*, *Jpn. Pat. Appl. 1-89151 (A)* (1987).
[5] D. R. de Sena, E. R. Gonzalez and E. A. Ticianelli, *Electrochim. Acta* **37** (1992) 1855.
[6] A. W. Adamson, 'Physical Chemistry of Surfaces', 4th edn., J. Wiley & Sons, New York (1982).
[7] V. A. Paganin, E. A. Ticianelli and E. R. Gonzalez, *J. Appl. Electrochem.*, **26** (1996) 297.

[8] E. A. Ticianelli, C. R. Derouin, A. Redondo and S. Srinivasan, *J. Electrochem. Soc.* **135** (1988) 2209.
[9] Y. W. Rho, O. A. Velev and S. Srinivasan, *J. Electrochem. Soc.* **141** (1994) 2084.
[10] Y. W. Rho and S. Srinivasan, *ibid.* **141** (1994) 2089.
[11] D. B. Sepa, M. V. Vojnovic and A. Damjanovic, *Electrochim. Acta* **32** (1987) 129.
[12] A. Parthasarathy, S. Srinivasan, A. J. Appleby and C. R. Martin, *J. Electrochem. Soc.* **139** (1992) 2856.
[13] D. R. de Sena, E. A. Ticianelli and E. R. Gonzalez, *J. Electroanal. Chem.* **357** (1993) 225.